www.lajss.org
Latin American Journal of Solids and Structures 3 (2006) 417–441

Plasticity-based constitutive model for concrete in stress space

Raveendra Babu R.[1], Gurmail S. Benipal[2,*] and Arbind K. Singh[3]

[1]Indian Institute of Technology Delhi, Department of Civil Engineering – India
[2]Indian Institute of Technology Delhi, Department of Civil Engineering – India
[3]Indian Institute of Technology Guwahati, Department of Civil Engineering – India

Abstract

The existing constitutive models of concrete elasto-plasticity are generally based on an assumed initial yield surface and on the unrealistic uniaxial stress-strain curves. In this paper, a new expression for the loading surface has been proposed and the model has been calibrated by using well established experimental data on failure and initial yielding of concrete. The evolution of loading surfaces with hardening involves their expansion and shape distortion. Analytical expressions for the plastic modulus for different choices of hardening parameter have been derived based on realistic uniaxial stress-strain curves with limited peak axial and lateral strains. Another distinctive feature of the approach followed is the choice of stress components as independent variables in the incremental constitutive equations. The empirical validity of the deduced failure criterion as well as the predicted material response under diverse stress histories has been evaluated. The general implications of the approach followed have also been delineated.

Keywords: concrete, hardening elasto-plasticity, loading surface, plastic modulus, stress space

1 Introduction

Concrete is modelled as a homogeneous isotropic nonlinear inelastic solid. Time-independent aspects of inelastic behaviour of concrete are generally modelled by assuming concrete to be a hardening elasto-plastic solid. The general theory of elasto-plasticity is developed by assuming initial and subsequent yield surfaces, loading-unloading criteria, flow rule and hardening rule. In general, the failure criteria have commonly been used for predicting the ultimate resistance of solid bodies and structures, the stress field being determined by assuming the material to be linear elastic up to the failure stage. Of course, some attempts have indeed been made to use failure criterion along with yield criterion to better model the evolution of loading surfaces during hardening [5, 6]. In such cases, the failure surface is supposed to constitute the outer bound of the loading surfaces in the stress space. These attempts include anisotropic hardening

*Corresp. author email: gurmail@civil.iitd.ac.in Received 7 April 2006; In revised form 4 October 2006

model of Mroz [13], hardening plasticity model of Chen and Chen [4], independent hardening model of Murray et al. [14], non-uniform hardening plasticity model of Han and Chen [8] and multiple hardening model of Ohtani and Chen [15], etc.

As concrete does not exhibit distinct yielding, there is a paucity of both the empirical data and the equations for initial yield surface of concrete. Still, the classical theory of elasto-plasticity assigns an arbitrarily chosen initial yield surface by modifying the shape as well as size of its failure surface [4, 7, 9, 14]. In an exceptional attempt, Launay and Gachon [11] have provided some qualitative description of the initial yield surfaces in the form of limit of crack initiation discontinuity and elastic limit without reference to the failure surface. However, the experimental data on the initial discontinuity curves in biaxial compression has been found to be incompatible with the theoretical predictions [4].

Development of subsequent yield surfaces or loading surfaces is controlled by a hardening function which, in turn, depends upon some hardening parameter incorporating history-dependence. The hardening parameters chosen by different researchers include effective plastic strain, plastic work, volumetric plastic strain, etc. One of the main assumptions of the classical elasto-plasticity theory is that the functional relation between the hardening function and hardening parameter and so, the plastic modulus, is same for all the strain/stress histories. Any one of the simpler load histories such as the uniaxial stress-strain curve for the material is used to uniquely establish this functional relation. Wherever the material response under uniaxial compressive stress has been used, it has been concluded from the available literature that the actual stress-strain curve for concrete under uniaxial compressive stress has rarely been used for predicting its inelastic response. In particular, the fact that concrete exhibits peak stress at a definite limited value of axial strain has totally been ignored. This is so despite the fact that there exists extensive experimental data and a number of equations like Madrid or Hognestad parabola and those due to Desai and Krishnan, Saenz, Tsai, Hinton and Owen, etc., concerning stress-strain curves for concrete under uniaxial compression [2].

The objective of the present paper is to construct the simplest hardening elasto-plasticity theory of concrete based upon sound empirical foundations. The proposed theory presumes a single empirically calibrated loading function incorporating strain/work hardening, associated flow rule and plastic modulus derived from realistic expressions for strains under uniaxial compressive stress test. Another distinctive feature of the proposed approach is the choice of stress components as independent variables. The attention is focused on delineating the various implications of this theory for the general hardening elasto-plasticity theory as well as its predictions of concrete behaviour under diverse stress histories. The scope of the paper is restricted to time-independent small deformations and the thermodynamic considerations, post-peak softening as well as stiffness degradation have not been incorporated.

2 Loading function

It is generally known that concrete is a pressure-sensitive solid which exhibits different behaviour in tension and compression. Also, the failure surface is open in the direction of the negative I_1-axis, whereas the initial yield surface as well as the loading surfaces are closed [11]. In view of these empirical facts, the following single general expression for the loading function has been proposed in terms of first invariant of the stress tensor I_1, second invariant of the stress deviator tensor J_2 and Lode angle θ:

$$f(I_1, J_2, \theta) = A\frac{J_2}{(f_c')^2} + \alpha\frac{\sqrt{J_2}}{f_c'} + B\frac{I_1}{f_c'} + C\frac{(I_1)^2}{(f_c')^2} - 1 = 0 \tag{1}$$

where $\cos 3\theta = \frac{3\sqrt{3}}{2}\frac{J_3}{J_2^{\frac{3}{2}}}$, $\alpha = [X\kappa\cos\theta + (1-\kappa)Y]$ and $C = C_0(1-\kappa)$.

Here, the parameters A, B, X, Y and C_0 are material constants. In the above equation, the parameters are normalized by using the uniaxial compressive strength of concrete $f_c^{'}$. The symbol κ denotes a hardening function of some hardening parameter like effective plastic strain, plastic work, etc. The evolution of the loading surfaces from initial yield to failure surface is governed by the changing value of the hardening function κ, its values at initial yield and failure being 0.3 and 1.0 respectively. The following failure criterion can be deduced from the loading function as a special case ($\kappa = 1.0$):

$$f(I_1, J_2, \theta) = A\frac{J_2}{(f_c')^2} + X\cos\theta\frac{\sqrt{J_2}}{f_c'} + B\frac{I_1}{f_c'} - 1 = 0 \tag{2}$$

For the purpose of calibration of the loading function, the parameters $f_c^{'}$ and $\sqrt{J_2}$ shall always be taken as positive. It is well known that the tensile strength is about 10 % of its compressive strength. Also, under equal biaxial compression, the strength of concrete is assumed to be 16 % higher than its uniaxial compressive strength [6, 10]. The material parameters A, B and X in equation (2) have been determined on the basis of the following three known failure states stated in terms of principal stresses (σ_1, σ_2 and σ_3).

1. Uniaxial compressive strength (0 / 0 / $-f_c^{'}$, $\theta = 60°$)
2. Uniaxial tensile strength ($0.1f_c^{'}$ / 0 / 0, $\theta = 0°$)
3. Biaxial compression (0 / $-1.16f_c^{'}$ / $-1.16f_c^{'}$, $\theta = 0°$)

These three states of stress at failure transform the equation (2) into the following three linear simultaneous equations in unknowns A, B and X.

1. $A + \frac{\sqrt{3}}{2}X - 3B = 3$
2. $A + 10\sqrt{3}X + 30B = 300$

3. $A + 0.8621\sqrt{3}X - 5.1724B = 2.2274$

By solving the above equations, the values of the empirical parameters A, B and X are obtained as 4.064147, 3.524653 and 10.980986 respectively.
Under uniaxial compression, concrete stress-strain curve is nearly linear elastic up to 30 % of its strength [5]. The last data point on the initial yield surface has been chosen in view of the fact that the concrete is linear elastic almost up to its failure in uniaxial tension. In view of this fact, it has been assumed here that concrete is linear elastic in uniaxial tension upto 90 % of its tensile strength. To determine the remaining material parameters C_0 and Y in equation (1), the following two stress states on initial yield surface ($\kappa = 0.3$) have been used:

4. Uniaxial compression (0 / 0 / $-0.3f_c^{'}$, $\theta = 60^{\circ}$)
5. Uniaxial Tension ($0.09f_c^{'}$ / 0 / 0, $\theta = 0^{\circ}$)

For these two states of stress at initial yield surface, the the equation (1) transforms into the following two linear simultaneous equations in unknowns C_0 and Y.

1. $C_0 + 1.9245Y = 26.7824$
2. $C_0 + 6.4148Y = 88.271$

By solving, the empirical constants C_0 and Y are obtained as 0.420382 and 13.698277 respectively.

3 Incremental constitutive equations

In the elastic range with $\kappa \leq 0.3$, concrete has been assumed to be an isotropic linear elastic solid and its constitutive equation is stated in incremental form as

$$d\epsilon_{ij}^{e} = D_{ijkl}^{e} d\sigma_{kl} \tag{3}$$

For $\kappa \geq 0.3$, the material undergoes elastic as well as plastic deformations. Decomposing the total strain increments into elastic and plastic increments, one obtains

$$d\epsilon_{ij} = d\epsilon_{ij}^{e} + d\epsilon_{ij}^{p} \tag{4}$$

The elastic strain increments are obtained from the above equation (3) whereas the plastic strain increments are obtained by using the associative flow rule as

$$d\epsilon_{ij}^{p} = d\lambda \frac{\partial f}{\partial \sigma_{ij}} \tag{5}$$

where the proportionality coefficient $d\lambda$ is a non-negative scalar. In general, the loading function is also stated as

$$f(\sigma_{ij}, \kappa) = 0 \tag{6}$$

The value of $d\lambda$ is determined from the following well known consistency condition:

$$df = \frac{\partial f}{\partial \sigma_{ij}} d\sigma_{ij} + \frac{\partial f}{\partial \kappa} d\kappa = 0 \tag{7}$$

The hardening function κ is uniquely determined by hardening parameter p. Thus, $\kappa = \kappa(p)$ and $d\kappa = H_p dp$, where H_p is plastic modulus of the material. The method of determination of H_p is given in the next section. In this paper, a new function h_p relating dp and $d\lambda$ is defined as $dp = h_p d\lambda$. Thus, the above consistency condition is rewritten as

$$df = \frac{\partial f}{\partial \sigma_{kl}} d\sigma_{kl} + h d\lambda = 0 \tag{8}$$

Thus,

$$d\lambda = \frac{-1}{h} \frac{\partial f}{\partial \sigma_{kl}} d\sigma_{kl} \tag{9}$$

where $h = \frac{\partial f}{\partial \kappa} H_p h_p$.

At any state of stress and the corresponding value of k exceeding 0.3, the stress increments resulting in positive value of $d\lambda$ constitute loading while its negative value implies unloading. The vanishing value of $d\lambda$ results in neutral loading.

In view of the above,

$$d\epsilon^p_{ij} = -\frac{1}{h} \frac{\partial f}{\partial \sigma_{ij}} \frac{\partial f}{\partial \sigma_{kl}} d\sigma_{kl} \tag{10}$$

The incremental constitutive equations can now be stated as

$$d\epsilon_{ij} = D^{ep}_{ijkl} d\sigma_{kl} \tag{11}$$

where D^{ep}_{ijkl}, the elasto-plastic compliance tensor given by $D^{ep}_{ijkl} = D^{e}_{ijkl} + D^{p}_{ijkl}$

$$D^p_{ijkl} = -\frac{1}{h} \frac{\partial f}{\partial \sigma_{ij}} \frac{\partial f}{\partial \sigma_{kl}} \tag{12}$$

Thus,

$$d\epsilon_{ij} = \left[D^e_{ijkl} - \frac{1}{h} \frac{\partial f}{\partial \sigma_{ij}} \frac{\partial f}{\partial \sigma_{kl}} \right] d\sigma_{kl} \tag{13}$$

The newly proposed function h_p depends upon the choice of the hardening parameter p. For various choices of the hardening parameters, such as effective plastic strain ϵ_p and plastic work W_p, the expressions for h_p have been deduced below:

When $p \equiv \epsilon_p$,

$$dp = d\epsilon_p = \sqrt{d\epsilon^p_{rs} \epsilon^p_{rs}} = d\lambda \sqrt{\frac{\partial f}{\partial \sigma_{rs}} \frac{\partial f}{\partial \sigma_{rs}}} = h_p d\lambda$$

$$h_p = \sqrt{\frac{\partial f}{\partial \sigma_{rs}} \frac{\partial f}{\partial \sigma_{rs}}} \tag{14}$$

When $p \equiv W_p$,

$$dp = dW_p = \sigma_{rs} d\epsilon^p_{rs} = \sigma_{rs} d\lambda \frac{\partial f}{\partial \sigma_{rs}} = d\lambda h_p$$

$$h_p = \frac{\partial f}{\partial \sigma_{rs}} \sigma_{rs} \tag{15}$$

For the determination of $d\lambda$, the remaining expression is written as

$$\frac{\partial f}{\partial \kappa} = \frac{\sqrt{J_2}}{f'_c} (X \cos\theta - Y) - \frac{C_0}{(f'_c)^2} (I_1)^2 \tag{16}$$

The following expression for κ in terms of stress components σ_{ij} will be found useful later:

$$\kappa = \frac{\frac{A}{(f'_c)^2} J_2 + Y \frac{\sqrt{J_2}}{f'_c} + B \frac{I_1}{f'_c} + C_0 \frac{I_1^2}{(f'_c)^2} - 1}{C_0 \frac{I_1^2}{(f'_c)^2} - \frac{\sqrt{J_2}}{f'_c} (X \cos\theta - Y)} \tag{17}$$

4 Hardening function and plastic modulus

The plastic modulus H_p can be expressed as

$$H_p = \frac{d\kappa}{dp} \tag{18}$$

The general elasto-plasticity theory is based on the assumption that the $\kappa - p$ relation is valid for all the stress histories. This relation, and so the expression for the plastic modulus, can be established from the known material response under some simple load history such as uniaxial compression test. In terms of $\sigma = -\sigma_{33}$, the expression for H_p can be stated as

$$H_p = \frac{d\kappa}{dp} = \frac{d\kappa}{d\sigma} \frac{d\sigma}{dp} \tag{19}$$

The state of uniaxial compressive stress ($\sigma_{33} = -\sigma$, all other stresses being absent) is characterized by $J_2 = \frac{\sigma^2}{3}$; $\sqrt{J_2} = \frac{\sigma}{\sqrt{3}}$; $I_1 = -\sigma$; and $\theta = 60^\circ$. In view of this, the loading function given in equation (1) reduces to the following relation between σ and κ

$$f = f(\sigma, \kappa) = \frac{A\sigma^2}{3(f'_c)^2} + \frac{\sigma \left(X\kappa \cos 60 + (1-\kappa)Y\right)}{\sqrt{3} f'_c} + \frac{B(-\sigma)}{f'_c} + \frac{C_0(1-\kappa)\sigma^2}{(f'_c)^2} - 1 = 0 \tag{20}$$

Using the numerical values of A, B, C_0, X, Y and f'_c (concrete strength is assumed as 20 MPa), the following explicit expression for σ in terms of κ has been obtained from the above equation.

$$\sigma = \frac{-(0.17596 - 0.161075\kappa) + \sqrt{0.0651 - 0.08376\kappa + 0.02595\kappa^2}}{0.01705 - 0.1345\kappa} \tag{21}$$

On differentiating the above expression, one obtains the following expression

$$\frac{d\kappa}{d\sigma} = \frac{0.1759 + 0.0171\sigma - \kappa(0.161075 + 0.01354\sigma)}{0.161075 + 0.00677\sigma^2} \tag{22}$$

For developing an analytical expression for the plastic modulus from the uniaxial compressive stress test, an expression for $\frac{d\sigma}{dp}$ has also to be stated in the analytical form. In this paper, the required expression has been developed for two choices (effective plastic strain ε_p and plastic work W_p) of the hardening parameter p. For this purpose, the axial strain as well as the lateral strains have to be expressed as functions of the applied axial stress. Traditionally, the material response under uniaxial compression is expressed in equations showing axial stress as a function of axial strain. One of the simplest expressions is Hognestad/Madrid parabola [3] stated in the following form

$$\sigma = f_c^{'}\left[\frac{2\epsilon}{\epsilon_0} - (\frac{\epsilon}{\epsilon_0})^2\right] \tag{23}$$

where σ and ϵ are axial compressive stress and strain respectively and ϵ_0 denote the strain at peak stress. As discussed above, it is more useful to express strain as function of stress as

$$\frac{\epsilon}{\epsilon_0} = 1 \pm \sqrt{1 - \frac{\sigma}{f_c^{'}}} \tag{24}$$

In these different versions of the parabola, both the stress and strain have been taken to be positive, even though they are known to be compressive, hence negative, variables. Also, the information about the lateral tensile strain is rarely available. The lack of such information is not felt by the researchers because of an additional assumption: Whenever the effective plastic strain is chosen as the hardening parameter, in uniaxial compression, it is assumed to be equal to the axial plastic strain. In the opinion of the authors of the present paper, this latter assumption imposes a very strong restriction on the model predictions and is without any known justification.

In this paper, the experimental data obtained form concrete under uniaxial compressive stress test have been used for evaluating the expression $\frac{d\sigma}{d\epsilon_p}$, but no restricting assumption like the one above has been made. Explicitly, the axial compressive plastic strain has not been assumed to represent the effective plastic strain in this paper. The justification for this assumption is provided later in this paper. In line with the sign convention adopted in the rest of the paper, the above expression is recast into the following form

$$\frac{\epsilon_{33}}{\epsilon_0} = -1 + \sqrt{1 + \frac{\sigma_{33}}{f_c^{'}}} \tag{25}$$

where σ_{33} and ϵ_{33} are the axial stress and strain respectively. It is well known that the peak strain is more or less constant for all grades of concrete and is generally assumed to be 0.002. In the above equation $f_c^{'}$ and ϵ_0 are positive quantities. Here, the stress-strain curve has been assumed to be of same form given above for all grades of concrete. At the elastic limit, $\sigma_{33} = -0.3f_c^{'}$, the equation (25) gives $\epsilon_{33} = -0.163\epsilon_0$. Thus, the Young's modulus of elasticity is determined

as $E_0 = \frac{\sigma_{33}}{\epsilon_{33}} = 1.8405\frac{f_c^{'}}{\epsilon_0}$.
In elastic range,

$$\frac{\epsilon_{33}^e}{\epsilon_0} = 0.543\frac{\sigma_{33}}{f_c^{'}} \tag{26}$$

In elasto-plastic range,

$$\frac{\epsilon_{33}^p}{\epsilon_0} = \frac{\epsilon_{33}}{\epsilon_0} - \frac{\epsilon_{33}^e}{\epsilon_0} \tag{27}$$

Thus,

$$\frac{\epsilon_{33}^p}{\epsilon_0} = -\left(1 + 0.543\frac{\sigma_{33}}{f_c^{'}}\right) + \sqrt{1 + \frac{\sigma_{33}}{f_c^{'}}} \tag{28}$$

and

$$d\epsilon_{33}^p = \frac{0.001086}{f_c^{'}}\left[-1 + \frac{0.9208103}{\sqrt{1 + \frac{\sigma_{33}}{f_c^{'}}}}\right] d\sigma_{33} \tag{29}$$

There is a scarcity of experimental data on the variation of lateral strain with axial stress in the uniaxial compressive stress test. From the available data [6], the lateral tensile strain $\bar{\varepsilon}$ corresponding to the peak stress has been estimated to be about 0.00075. Like the axial compressive strain ε_0 at peak stress, the corresponding lateral strain $\bar{\varepsilon_0}$ has been assumed to be independent of the concrete grade. However, the actual values of ε_0 and $\bar{\varepsilon_0}$ can easily be incorporated in the proposed model. In the absence of any lateral strain-axial stress relations in the literature, in this paper, the variation of axial as well as lateral strains with stress has been assumed to be of the same form. Poisson's ratio has been assumed to be 0.2. In view of this, the lateral strain at the elastic limit are obtained as $0.2\times0.163\epsilon_0 = 0.0326\times2000\times10^{-6} = 65.2\times10^{-6}$. As in the case of axial strain, the lateral elastic strains are related to axial stress as

$$\frac{\epsilon_{11}^e}{\bar{\epsilon_0}} = \frac{\epsilon_{22}^e}{\bar{\epsilon_0}} = -0.2896\frac{\sigma_{33}}{f_c^{'}} \tag{30}$$

The axial stress-lateral strain relation is assumed to be of the form

$$\frac{\sigma}{f_c^{'}} = a\frac{\epsilon}{\bar{\epsilon_0}} + b\left(\frac{\epsilon}{\bar{\epsilon_0}}\right)^2 \tag{31}$$

The empirical constants a and b are determined from the condition that the lateral strains at compressive stress values of $0.3f_c^{'}$ and $f_c^{'}$ respectively are 65.2×10^{-6} and 0.00075. The values of a and b are obtained as 3.68643 and -2.68643 respectively. Thus, the above equation (31) is rewritten as

$$\frac{\sigma}{f_c^{'}} = 3.68643\frac{\epsilon}{\bar{\epsilon_0}} - 2.68643\left(\frac{\epsilon}{\bar{\epsilon_0}}\right)^2 \tag{32}$$

The lateral strain is related to the axial stress by the equation

$$\frac{\epsilon}{\bar{\epsilon_0}} = 0.68612\left[1 - \sqrt{1 - 0.79072\frac{\sigma}{f_c^{'}}}\right] \tag{33}$$

In terms of $\epsilon_{11}, \epsilon_{22}$ and σ_{33}, the above equation is restated as

$$\frac{\epsilon_{11}}{\bar{\epsilon_0}} = \frac{\epsilon_{22}}{\bar{\epsilon_0}} = 0.68612 \left[1 - \sqrt{1 + 0.79072 \frac{\sigma_{33}}{f_c'}}\right] \tag{34}$$

The lateral plastic strain components are obtained below:

$$\frac{\epsilon_{11}^p}{\bar{\epsilon_0}} = \frac{\epsilon_{22}^p}{\bar{\epsilon_0}} = \frac{\epsilon_{11}}{\bar{\epsilon_0}} - 0.2896 \frac{\sigma_{33}}{f_c'} \tag{35}$$

Using the equations (34) and (35), one obtains the following expression

$$d\epsilon_{11}^p = d\epsilon_{22}^p = \frac{0.00022}{f_c'} \left[1 - \frac{0.9366865}{\sqrt{1 + 0.79072 \frac{\sigma_{33}}{f_c'}}}\right] d\sigma_{33} \tag{36}$$

Substituting the expressions (36) and (29) for $d\epsilon_{11}^p, d\epsilon_{22}^p$ and $d\epsilon_{33}^p$ in the equation,

$$d\epsilon_p = \sqrt{(d\epsilon_{11}^p)^2 + (d\epsilon_{22}^p)^2 + (d\epsilon_{33}^p)^2} \tag{37}$$

It is clear from the above equation that, as ε_{11}^p and ε_{22}^p are non-zero, the effective plastic strain ε_p is always distinct from the axial plastic strain ε_{33}^p in uniaxial compression. Thus, the assumption to this effect made earlier in the paper stands vindicated. Using the equations (29), (36) and (37), one obtains the following expression:

$$\frac{d\sigma}{dp} = \frac{d\sigma_{33}}{d\epsilon_p} = \frac{f_c'}{\sqrt{1.2737 \times 10^{-6} + \frac{8.27827 \times 10^{-8}}{1 + 0.79072 \frac{\sigma_{33}}{f_c'}} + \frac{0.999999 \times 10^{-6}}{1 + \frac{\sigma_{33}}{f_c'}} - \frac{17.675 \times 10^{-8}}{\sqrt{1 + 0.79072 \frac{\sigma_{33}}{f_c'}}} - \frac{2.172 \times 10^{-6}}{\sqrt{1 + \frac{\sigma_{33}}{f_c'}}}}} \tag{38}$$

When plastic work W_p is chosen as the hardening parameter, the required expression for $\frac{d\sigma}{dp}$ is obtained by following similar procedure. In the uniaxial case,

$$dW_p = \sigma_{33} d\epsilon_{33}^p \tag{39}$$

$$\frac{d\sigma}{dp} = \frac{-d\sigma_{33}}{dW_p} = \frac{-1}{\sigma_{33}\epsilon_0 \left(\frac{-0.543}{f_c'} + \frac{1}{2f_c'} \frac{1}{\sqrt{1 + \frac{\sigma_{33}}{f_c'}}}\right)} \tag{40}$$

5 Computational algorithm

In this paper, the material response is measured in terms of strains while the stress components are chosen to play the role of independent variables. At any stage of the loading process, the

state of system is known in terms of the stresses and strains and it is desired to obtain the incremental strain response to the applied stress increments. For achieving this, the following computational algorithm is adopted:

The hardening function κ is evaluated in terms of the known stress components. If κ does not exceed κ_y, i.e., the maximum value of the κ reached in the past, then the material is in the elastic range and the elastic strain increments are obtained by using equation (3). Otherwise, the material is in the elasto-plastic range and the response can be determined by first computing the value of D^{ep}_{ijkl}. For doing so, the required values of the expressions $\frac{\partial f}{\partial \sigma_{ij}}$, $\frac{\partial f}{\partial k}$ and h_p are determined in terms of known values of σ_{ij} and κ.

For quantifying the value of the plastic modulus H_p, first the expressions $\frac{dk}{d\sigma}$ and $\frac{d\sigma}{dp}$ have to be evaluated. The former is known in terms of κ from expression (22) and the latter expression is known in terms of σ_{ij} and κ for the chosen hardening parameter p. Having determined the D^{ep}_{ijkl} components, the strain increments $d\epsilon_{ij}$ can be evaluated in terms of applied stress increments $d\sigma_{kl}$. These stress and strain increments are then used to establish the new states of stress and strain. The same procedure is adopted for obtaining the material response to any stress history. A MATLAB [1] program has been developed to implement the above algorithm. Derivatives of the proposed loading function required for computational purposes have been provided in the Appendix.

6 Discussion and interpretation

In this paper, a new expression for the loading function has been proposed for hardening elasto-plastic behaviour of concrete. The evolution of loading surfaces from the initial yield surface to the failure surface is governed by the load history incorporated in the equation in the form of hardening function κ.

For the limiting case of the failure surface ($\kappa = 1$), the equation for the proposed loading surface assumes a form similar to that of Ottosen failure criterion as can be seen from equations (1) and (2). The deduced failure criterion is a three parameter criterion calibrated by three known states of stress at failure. Concrete is a pressure-sensitive material, its meridians in the Haigh-Westergaard stress-space for different values of θ are curved and its failure surface is open in the direction of negative hydrostatic axis. As shown in figures (1), (2) and (3), the failure criterion deduced from the proposed loading surface meets all the above general requirements. Additionally, the deviatoric sections change from roughly triangular shape for lower absolute values of first stress invariant to more or less circular shape for very high absolute values [6]. Computations based upon the proposed failure criterion seem to confirm this empirical observation. For example, for values of I_1 equal to 0 and 87, the values of $\sqrt{2J_2}$ for tension and compression meridians turns out to be 0.56 and 0.9 respectively. The predictions of the deduced failure criterion are in close agreement with those of the Ottosen failure criterion as shown in

[1] MATLAB is a registered trademark of The MathWorks, Inc.

table (1) and figure (1).

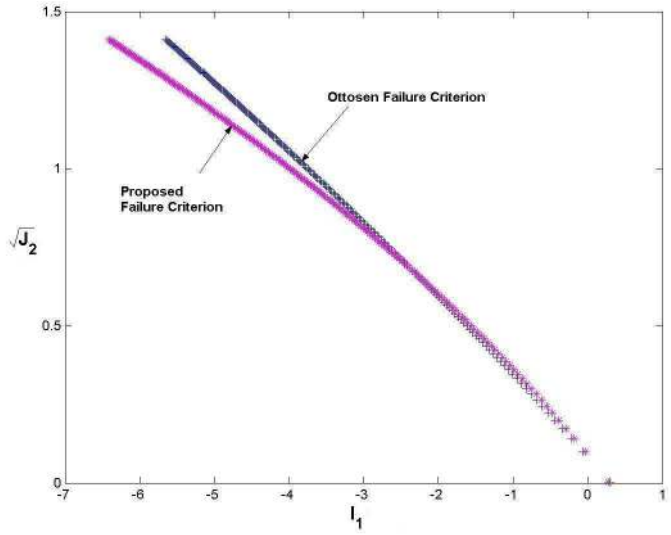

Figure 1: Comparison of proposed failure criterion with Ottosen criterion

	UC(σ_{33})	UT(σ_{11})	BC($\sigma_{22}=\sigma_{33}$)	PS($\sigma_{11}=-\sigma_{33}$)	HC(σ_m)	HT(σ_m)
Failure Surface						
Ottosen	$-0.9993f_c^{'}$	$0.1f_c^{'}$	$-1.161f_c^{'}$	$0.0937f_c^{'}$	∞	$0.0996f_c^{'}$
Proposed	$-0.999999f_c^{'}$	$0.1f_c^{'}$	$-1.160014f_c^{'}$	$0.100811f_c^{'}$	∞	$0.09456f_c^{'}$
Initial Yield Surface						
Proposed	$-0.297176f_c^{'}$	$0.090213f_c^{'}$	$-0.727582f_c^{'}$	$0.078319f_c^{'}$	$-4.08367f_c^{'}$	$0.09241f_c^{'}$
UC: Uniaxial Compression; UT: Uniaxial Tension; BC: Biaxial Comp.; PS: Pure Shear HC: Hydrostatic Compression; HT: Hydrostatic Tension						

Table 1: Predictions from the proposed loading surface

The proposed loading surfaces resemble in form those proposed by Han and Chen [8]. In particular, the initial yield corresponds to a value of 0.3 of the hardening function κ. The evolution of the loading surfaces has been traced in triaxial as well as biaxial states of stress and compared with the data available in literature [10, 12] as shown in figures (2) and (3). It can be observed from these figures that the inelastic zone between initial yield and failure is smaller under predominant tension and expands as compression dominates. This is as per expectations from this quasi-brittle solid.

The newly proposed function h_p of the stresses and κ depends upon the choice of the hardening parameter. The introduction of this function has made it possible to employ the same expression (equation 9) for $d\lambda$ for all choices the hardening parameter like effective plastic strain

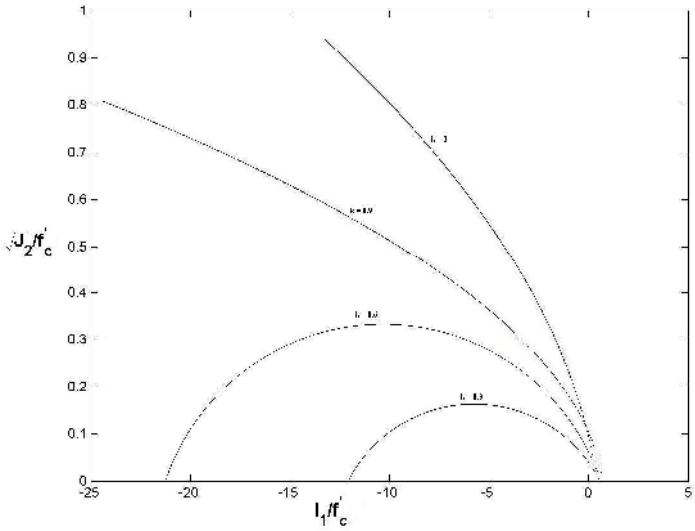

Figure 2: Evolution of loading surfaces

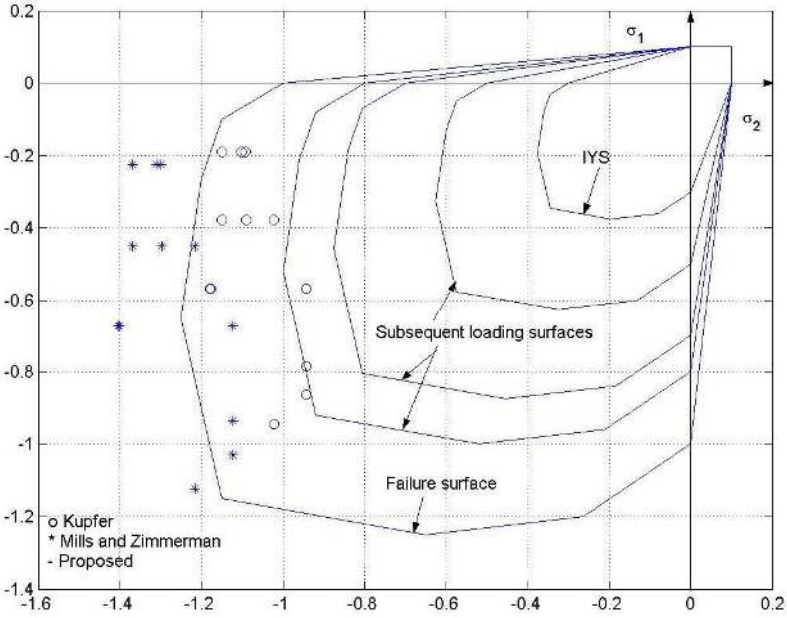

Figure 3: Evolution of loading surface in plane stress case

and plastic work.

Following the common practice, universal $\kappa - p$ relation is obtained from the uniaxial compressive stress test. In this paper, κ is expressed as a function of σ representing absolute value of σ_{33} which, in turn, is expressed as a function of p. The required expressions for the axial as well as lateral strains in terms of axial stress have been derived from the Madrid Parabola. The expressions for $\frac{d\sigma}{dp}$ have been derived for different choices of hardening parameter. Also, using the equation (22), the expression $\frac{dk}{d\sigma}$ can be evaluated. In this manner, the corresponding explicit analytical expressions for the plastic modulus have been derived. The variation of $\kappa - \epsilon_p$ and $\kappa - W_p$ as well as the corresponding variation of H_p with k has also been plotted in figures (4) and (5).

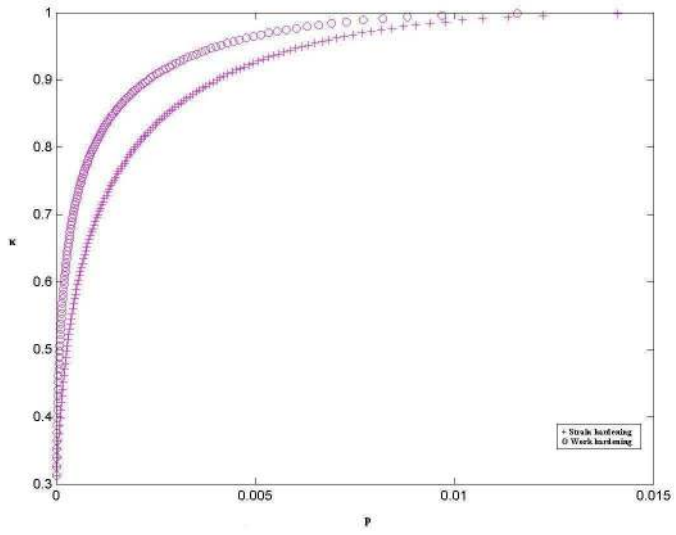

Figure 4: Hardening function

It can be seen that the plastic modulus vanishes asymptotically as the failure stage is reached, i.e., when $\kappa \to 1$. Because of the fact that the parameter H_p appears in the denominator of their expressions, the elasto-plastic compliance tensor components can be expected to attain infinitely high values asymptotically as failure stage is approached. This implies that the corresponding tangent elasto-plastic stiffness tensor components as well as its eigen values vanish asymptotically. This results in the loss of positive definite character of this stiffness tensor of the material marking the onset of instability of its equilibrium states. Such a loss of material stability has been interpreted as constituting elasto-plastic failure [1]. As such states of stress are infinitely close to the failure surface, only the infinitely small stress increments are admissible and the strain increments at failure are of limited magnitude only. This implies that the failure is predicted to occur at limited values of peak strain. For example, for the case of unequal biaxial compression, the values of the principal strains at stresses very close to failure (at $\kappa = 0.998823$)

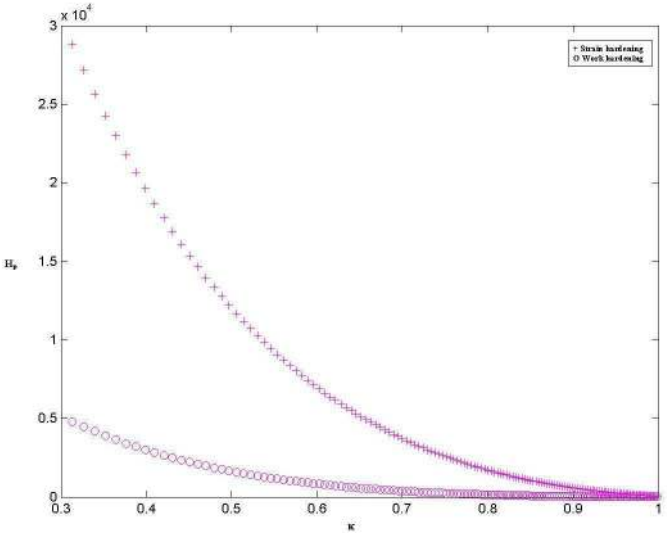

Figure 5: Variation of plastic modulus with hardening function

are obtained as $0.00395133, -0.00080503$ and -0.00249828 respectively. Obviously, such strain values can not be termed as infinitely large.

In view of the equation (2), the failure of concrete is predicted to be stress-path independent, even though the load path has been observed to affect the strength of concrete to a limited extent. Even at the risk of sounding repetitive, it should be appreciated that failure of concrete is predicted to occur as and when κ approaches unity. Since the $\kappa - p$ relation is unique and monotonic, the failure is predicted to occur as and when a maximum value of the chosen hardening parameter is reached. Following the common practice of classifying failure criteria, concrete can be said to obey maximum effective plastic strain criterion or maximum plastic work criterion, etc., depending on the choice of the hardening parameter made.

Concrete, an isotropic nonlinear elasto-plastic solid, exhibits some aspects of the incremental mechanical behaviour resembling that of isotropic nonlinear elastic solids. These aspects include stress-induced anisotropy, coaxiality of principal stresses and strains, normal 'stress effect', etc,. For any general state of stress, as the values of $\frac{\partial f}{\partial \sigma_{11}}$, $\frac{\partial f}{\partial \sigma_{22}}$ and $\frac{\partial f}{\partial \sigma_{33}}$ in equation (12) are different, the tangent plastic compliance tensor components D^p_{1111}, D^p_{2222} and D^p_{3333}, and so the corresponding elasto-plastic compliance tensor components $D^{ep}_{1111}, D^{ep}_{2222}$ and D^{ep}_{3333}, are all different implying stress-induced anisotropy. It has been verified that principal stresses introduce only normal strains and no shear strains. This happens because, in such cases, the expression $\frac{\partial f}{\partial \sigma_{rs}}$ for $r \neq s$ vanishes. Thus, isotropic elasto-plastic solids also exhibit coincidence of principal stress and strain axes. If two of the principal stresses are same, then the principal strains in these two direction are also equal. However, application of any shear stress component, say σ_{23}, introduces normal strains in all directions in addition to the corresponding shear strain ϵ_{23} but

other shear strains ϵ_{12} or ϵ_{31} are not introduced. The plastic Poisson's ratio or the coefficient of contraction under uniaxial compressive stress comes out to be the ratio of $\frac{D^p_{1133}}{D^p_{3333}}$ and it varies with the magnitude of stress.

Using the proposed incremental constitutive equations, the material response under diverse monotonic proportional stress histories has been obtained for two different choices of hardening parameter. The stress histories investigated include uniaxial compression (figure 6), equal and unequal biaxial compression (figure 7 and figure 8), triaxial compression (figure 9), uniaxial tension (figure 10) and pure shear (figure 11). At lower values of the hardening function, higher strains are predicted for strain hardening. The difference between strain hardening and work hardening models is explained by the lower values of the plastic modulus in strain hardening at lower values of κ as shown in figure (5). The theoretical predictions for uniaxial compression as well as equal and unequal biaxial compression have been compared with Kupfer's experimental data [10]. It can be observed from relevant figures that theoretical predictions for all these cases are quite satisfactory.

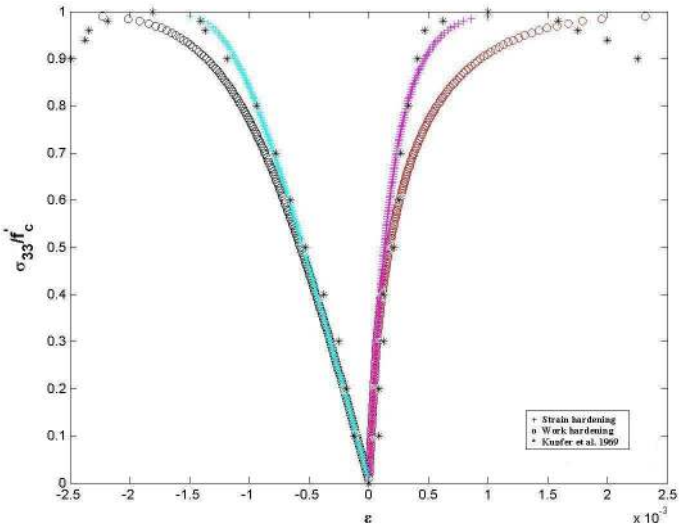

Figure 6: Uniaxial compression response (0/0/-1)

For all stress histories, as failure approaches, the stress-strain curves progressively become more flat thus implying peak failure stress at definite strain values. As shown in the relevant figures, under uniaxial tension and pure shear, where tensile stress dominates, the initial yielding is predicted to occur at stress levels approaching failure. This observation confirms quasi-brittle material response in such states of stress in contrast to those cases with dominant compression. Experimental investigations have revealed the occurrence of dilatant behaviour in concrete under uniaxial compression as well as equal and unequal biaxial compression. The predicted response shown in figure (12) both for strain hardening and work hardening simulates such observed

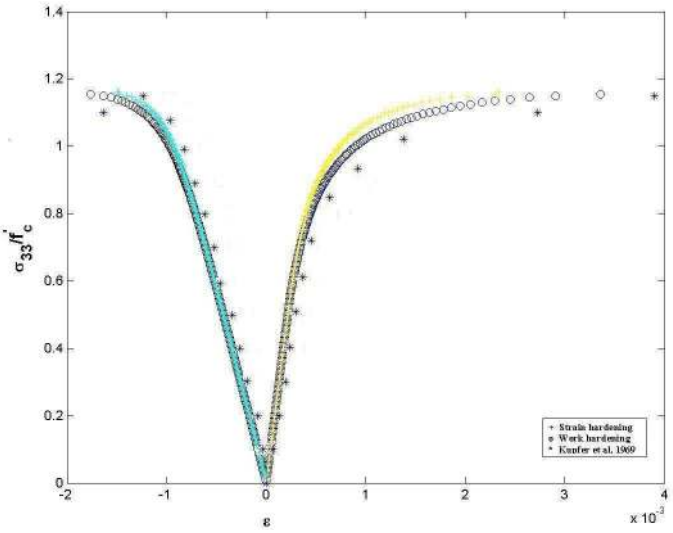

Figure 7: Eqi-biaxial compression response (0/-1/-1)

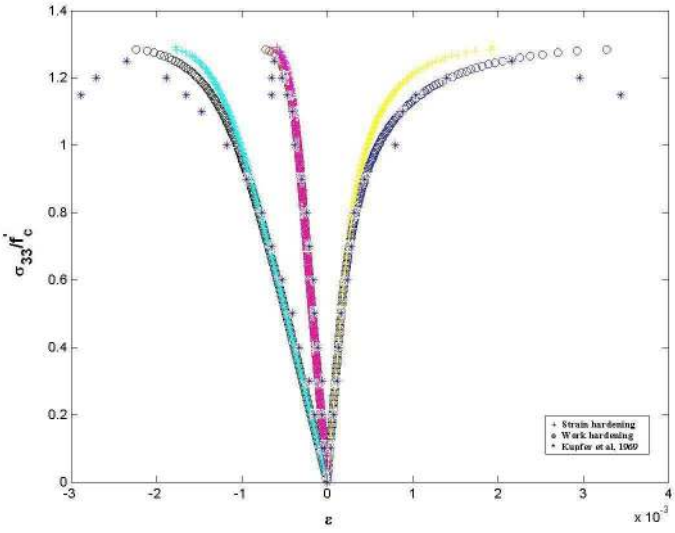

Figure 8: Unequal biaxial compression response (0/-0.52/-1)

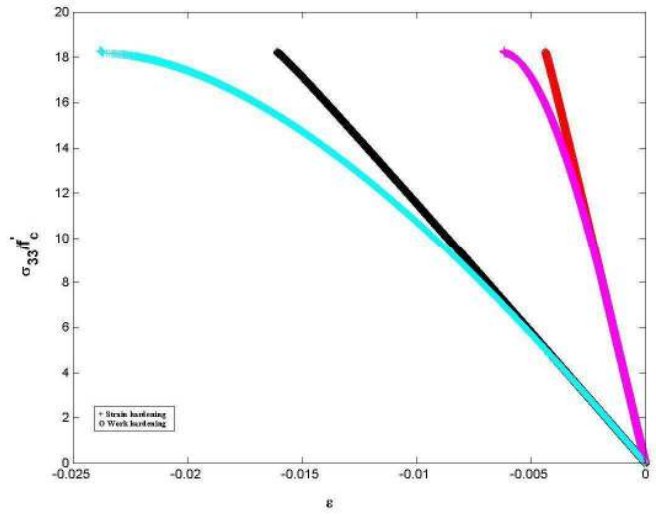

Figure 9: Triaxial compression response (-0.52/-0.52/-1)

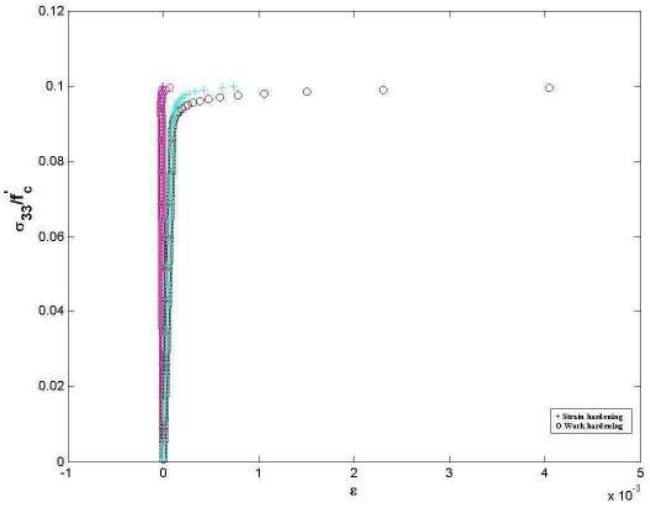

Figure 10: Uniaxial tension response (0/0/1)

behaviour satisfactorily [5]. For example, in all these cases, the volume keeps on decreasing with increase in stress and reaches a minimum value at stress levels varying in the range of about 80 to 90 % of the corresponding failure stress. The shape itself of the loading surfaces near failure stage implies only dilatant incremental plastic response.

The present theory is also capable of predicting concrete response under repeated loading/unloading cycles, stress reversal and non-proportional load paths. The theoretical predica-

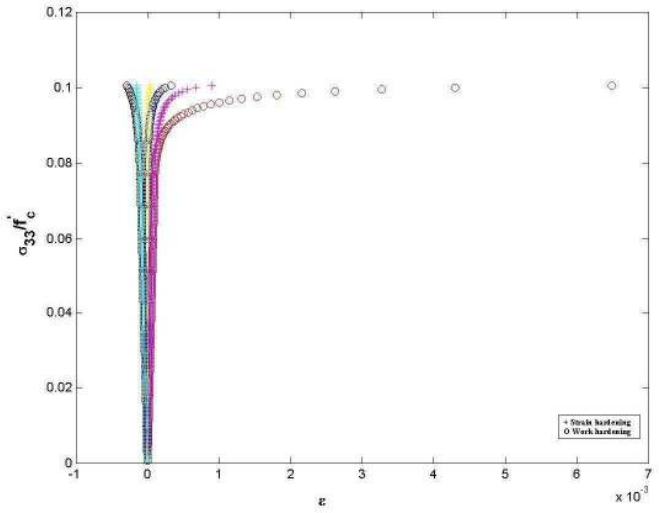

Figure 11: Pure shear response (0/1/-1)

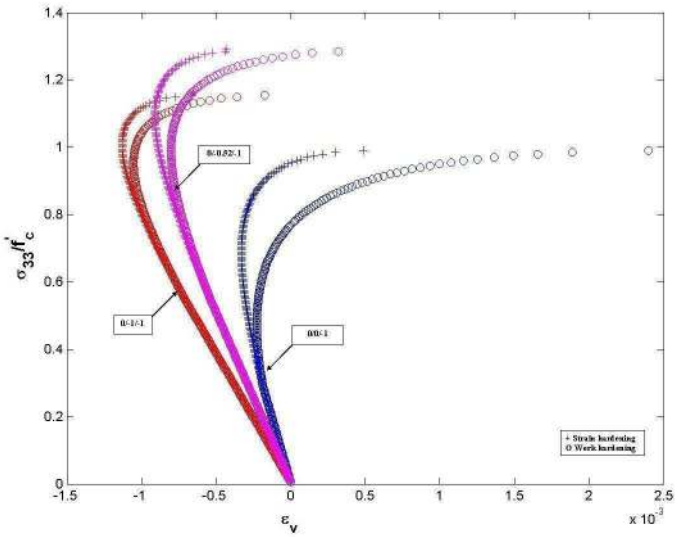

Figure 12: Volumetric strain response

tions of concrete behaviour under repeated loading/unloading cycles under uniaxial compressive stress has been shown in figure (13). Effect of pre-loading in uniaxial compression beyond the initial yield surface on the behaviour under uniaxial tension and on further reloading in uniaxial compression has been shown in figure (14). Also, the theory is shown, in figure (15), to predict the effect of a loading/unloading cycle in uniaxial compression on the behaviour of concrete under subsequent loading in uniaxial compression in the lateral direction. In view of the fact

that all the loading surfaces excluding the failure surface are closed, the concrete is expected to exhibit irreversible mechanical behaviour even under hydrostatic compression. The same has been investigated and it has been found that the predicted plastic strains are infinitesimally small. Thus, the material response to hydrostatic pressure is predicted to be predominantly elastic in nature.

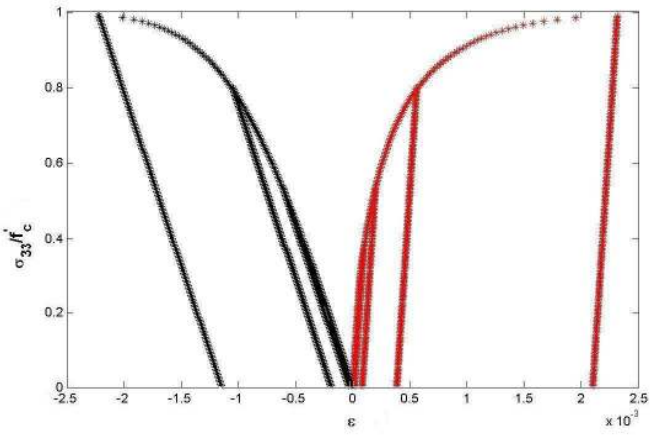

Figure 13: Loading unloading cycles in uniaxial compression

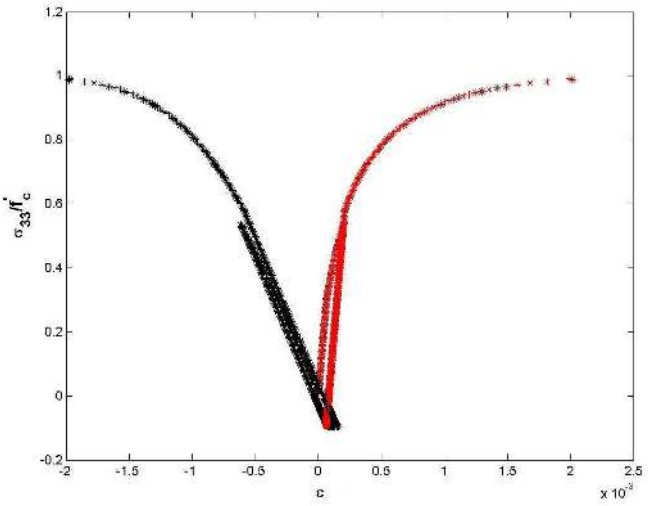

Figure 14: Stress reversal

As is the common practice, the loading surfaces from the initial yield to the failure are defined in the stress space. However, in this paper, the stress components play the role of the primary variables. Such a choice is motivated by the fact that, almost invariably, the experimental data

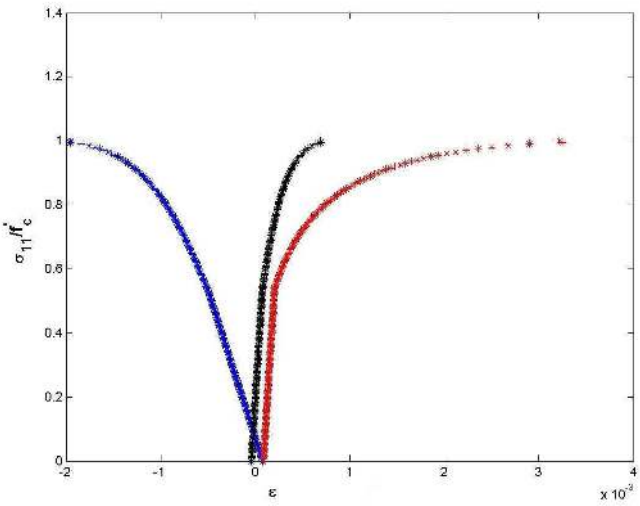

Figure 15: Effect of pre-loading (σ_{33}) on response under uniaxial compression (σ_{11})

concerning the failure as well as stress-strain curves of concrete is obtained by varying stress tensor components in a monotonic proportional manner. Thus, the evolution of loading surfaces is controlled by the chosen stress increments. The proposed numerical integration algorithm does not demand cumbersome iterations. The chosen hardening parameter does not need to be quantified at any stage. In contrast, in the conventional hardening elasto-plasticity theories, the evolution of loading surface is controlled by the hardening function in turn dependent upon the current value of the chosen hardening parameter.

As argued above, the hardening function, the chosen hardening parameter, plastic modulus and the tangent elasto-plastic compliance tensor components all are determined uniquely by the instantaneous state of stress. In other words, these are the state variables in the stress space implying their stress-path independence. In contrast, the plastic strains, and so the total strains, exhibit stress path dependence. However, the values of strains corresponding to any specified state of stress are independent of the monotonic stress histories. Within the acceptable computational error, this claim has been verified to be valid for different stress histories. For example, concrete was first loaded under equal biaxial compression upto stress level of -14.45 MPa following proportional load path. Then, one of the compressive stresses was increased to -19.58 MPa without changing the other stresses thus following a monotonic non-proportional load path. The normal strains were obtained as $0.00054981, -0.00059634$ and -0.0009463. The same final state of stress $(0/-14.45/-19.58)$ was attained following proportional load path and the corresponding state of strain was obtained as $0.00057161, -0.00058937$ and -0.00095971. Similarly, the change in strains in the material associated with change from one state of stress to another turns out to be the same for all monotonic stress paths followed. The same is true for the plastic work, and so the total work done on the material.

Thus, the proposed flow theory of elasto-plasticity is equivalent to a deformation theory. In contrast to earlier research, such an equivalence is not restricted only to proportional stress paths. Such stress-path independence of strains is also implied by the path-independence of the hardening function κ as well as hardening parameter p and their unique determination by the current state of stress on the current loading surface. It should be appreciated that the load-history affects the elaso-plastic response only through its effect on the hardening parameter and so on the hardening function. For any specified state of stress, all load histories are equivalent in that they yield the same value of p and κ. Such path-independence in the stress space does not imply the same in the strain space.

As is well known, the Drucker's stability postulates are guaranteed by the convexity of the loading surfaces and the associative flow (normality) rule. These postulates also imply continuity and uniqueness of the material response as well as symmetry of the elasto-plastic compliance tensor. In contrast, the use of non-associative flow rule and the asymmetric compliance tensor imply uniqueness of strain trajectory corresponding the specified stress history [5]. In this paper, associative flow rule has been used and so the uniqueness of the strain response for every state of stress is achieved. It has been argued above that the material response in the present case is independent of the monotonic stress histories. Such path-independence is restricted only to monotonic loading because of the irreversible deformations associated with unloading.

At this point, the distinction between irreversibility of material response and its path dependence or otherwise should be appreciated. The notion of irreversible or inelastic response refers to the case when, after loading-unloading cycles, the system does not revert to its earlier state before loading. During such closed load cycles, the inelastic material exhibits irreversible plastic strains as well as energy dissipation. In contrast, the material response is said to be path independent if the strain corresponding to a specified state of stress is independent of the load (stress) history. Path independence of material response during monotonic loading is associated with the symmetry of the tangent elasto-plastic compliance tensor, while the irreversibility during general stress variations is due to difference in the values of compliance tensor components during loading and unloading. As is the case with the material studied in this paper, the material can simultaneously exhibit both irreversible and path independent response. After all, the material response under uniaxial stress routinely used for obtaining plastic modulus is stated without reference to any load history.

Even though, in the theories of concrete elasto-plasticity, the loading function is almost invariably stated in terms of stresses, the choice of the stress components as independent variables has rarely been made [16]. This is because of compatibility of strain components as primary variables with computational elasto-plasticity employing displacement based finite element formulation. Using the proposed expressions for the loading function and the plastic modulus, the incremental constitutive equations can easily be restated with strain components as the primary variables [5]. Even though, in the currently dominant computational paradigm, the strain components are preferred to play the role of independent variables for solving boundary value problems, such a choice has the unfortunate consequence of causing conceptual confu-

sion, e.g., concerning the distinction between irreversibility and path-dependence of material response. It should be appreciated that while computation is important for its applications, only the analytical approach reveals the structure of the elasto-plasticity theory.

The primary aim of the dominant contemporary elasto-plasticity theories is the successful prediction of the observed empirical material response using any pragmatic approach. A case in point involves three different models [4, 8, 15] of loading surfaces which have been shown to satisfactorily predict the same empirical data. In contrast, apart from predicting the observed material behaviour, an attempt has been made in this paper to establish the basic characteristic features of the proposed elasto-plasticity theory.

7 Conclusions

In this paper, a new single expression for the loading function has been proposed and calibrated with established empirical data. The loading surfaces coincide with the initial yield surface as the inner limit surface and with the failure surface as the outer limit surface. The deduced failure criterion has been found to predict satisfactorily the failure of concrete under diverse states of stress. As has been argued in the paper, concrete can be said to obey maximum effective plastic strain criterion or maximum plastic work criterion. The material failure has been shown to occur at peak stress occurring at definite values of strain components and so to constitute elasto-plastic failure.

The loading surfaces evolve during hardening by expansion and shape distortion. Their evolution is controlled by the chosen stress path. Also, using uniaxial compression test data, explicit analytical expressions have been derived for the plastic modulus for different choices of hardening parameter. Convexity of the proposed loading surfaces along with associative flow rule guarantees the uniqueness and stability of the material response as per Drucker's stability postulates.

Using the derived incremental elasto-plastic constitutive equations, the proposed theory has been applied for predicting the material response to various stress histories involving monotonic proportional loading, loading-unloading cycles, stress reversals and change of direction of uniaxial compressive stress. The predicted response has been found to be satisfactory. Also, concrete is predicted to exhibit coaxiality of principal stresses and strains, stress-induced anisotropy, normal stress effects, dilatancy under uniaxial and biaxial compression, predominantly elastic behaviour under hydrostatic compression, and quasi-brittle behaviour under tension and pure shear.

A distinctive feature of the present paper is the choice of stresses as independent variable resulting in simpler non-iterative computational algorithm. It has been argued that the material response including its failure is independent of monotonic stress histories. Such path independence differs from irreversibility under general stress variations involving loading-unloading. The cause of such path independence in stress space is the fact that the hardening function, the hard-

ening parameter, plastic modulus and the tangent elasto-plastic compliance tensor components are state variables in that space.

The proposed theory incorporates the basic minimal aspects of the elasto-plasticity theory and has been calibrated by using commonly known experimental data on initial yield and failure of concrete as well as its response in the uniaxial compressive stress test. In this 'rational' theory, no additional empirical constants or expressions have been used. In particular, unlike the current empirical theories, no attempt has been made to force compatibility of theoretical predictions with empirical data by using some pragmatic empirical techniques. The hardening time-independent elasto-plasticity theories like the present one are not expected to predict stiffness degradation and creep failure at sufficiently elevated stress levels exhibited by concrete. This fact should be kept in mind while evaluating the empirical validity of such theories. In this paper, the implications of the underlying assumptions have been worked out exposing the strengths as well as the weaknesses of the theory. It is believed that only by proceeding in this manner can better theories of concrete elasto-plasticity be constructed.

References

[1] R. R. Babu and Gurmail S. Benipal. Elasto-plastic failure of concrete. In *Proc. Indian Society of Theoretical and Applied Mechanics*, pages 66–74, 2005.

[2] R. R. Babu, Gurmail S. Benipal., and A. K. Singh. Constitutive modelling of concrete: an overview. *Asian. J. of Civil Engrg.*, 6(4):211–246, 2005.

[3] M. Cervera and E. Hinton. Nonlinear analysis of reinforced concrete plates and shells using a three dimensional model. In E. Hinton and R. Owen, editors, *Comp. Modeling of RC struct.*, pages 327–370. Pineridge Press, UK, 1986.

[4] A. C. T. Chen and W. F. Chen. Constitutive relations for concrete. *J. Engrg. Mech., ASCE*, 101(4):465–481, 1975.

[5] W.F. Chen. *Constitutive equations for engineering materials, Vol. 2: Plasticity and modelling.* Elsevier Publications, 1994.

[6] W.F. Chen and A. F. Saleeb. *Constitutive equations for engineering materials Vol. 1: Elasticity and modelling.* Elsevier Publications, 1994.

[7] P. Grassl, K. Lundgren, and K. Gylltoft. Concrete in compression: a plasticity theory with novel hardening law. *Int. J. Solids Struct*, 39:5202–5223, 2002.

[8] D. J. Han and W. F. Chen. A nonuniform hardening plasticity model for concrete materials. *Mechanics Of Materials.*, 4(4):283–302, 1985.

[9] I. Imran and S.J. Pantazopoulou. Plasticity model for concrete under triaxial compression. *J. Engrg. Mech., ASCE*, 127(3):281–290, 2001.

[10] H. Kupfer, H. K. Hilsdorf, and H. Rush. Behavior of concrete under biaxial stresses. *ACI Journal*, 66(8):656–666, 1969.

[11] P. Launay and H. Gachon. Strain and ultimate strength of concrete under triaxial stresses. *SP-34 ACI. J.*, 1:269–282, 1970.

[12] L.L. Mills and R.M. Zimmerman. Compressive strength of plain concrete under multiaxial loading conditions. *ACI. J.*, 67(10):802–807, 1970.

[13] Z. Mroz. On the description of anisotropic work-hardening. *J. Mech. Phys. Solids*, 15(163), 1967.

[14] D. W. Murray, L. Chitnuyanondh, K. Y. Rijub-Agha, and C. Wong. Concrete plasticity theory for biaxial stress analysis. *J. Engrg. Mech., ASCE*, 105(6):989–1006, 1979.

[15] Y. Ohtani and W. F. Chen. Multiple hardening plasticity for concrete materials. *J. Engrg. Mech., ASCE*, 114(11):1890–1910, 1988.

[16] J. C Simo and T. J. R Hughes. *Computational Inelasticity*. Springer-Verlag, NY, 1998.

Appendix: Derivatives of the proposed loading function

$$\frac{\partial f}{\partial \sigma_{ij}} = \frac{A}{(f_c')^2}\frac{\partial J_2}{\partial \sigma_{ij}} + \frac{\alpha}{f_c'}\frac{\partial \sqrt{J_2}}{\partial \sigma_{ij}} + \frac{\sqrt{J_2}}{f_c'}\frac{\partial \alpha}{\partial \sigma_{ij}} + \frac{B}{f_c'}\frac{\partial I_1}{\partial \sigma_{ij}} + \frac{2CI_1}{(f_c')^2}\frac{\partial I_1}{\partial \sigma_{ij}} \tag{A.1}$$

$$\frac{\partial J_2}{\partial \sigma_{ij}} = S_{ij} \tag{A.2}$$

$$\frac{\partial \sqrt{J_2}}{\partial \sigma_{ij}} = \frac{1}{2\sqrt{J_2}} S_{ij} \tag{A.3}$$

$$\frac{\partial I_1}{\partial \sigma_{ij}} = \delta_{ij} \tag{A.4}$$

$$-\sin 3\theta \frac{\partial \theta}{\partial \sigma_{ij}} = \frac{\sqrt{3}}{2}\left[\frac{-3}{2}\frac{J_3}{J_2^{\frac{5}{2}}}S_{ij} + \frac{1}{J_2^{1.5}}\left(S_{ik}S_{kj} - \frac{2}{3}J_2\delta_{ij}\right)\right] \tag{A.5}$$

$$\frac{\partial \theta}{\partial \sigma_{ij}} = -\frac{\sqrt{3}}{2\sin 3\theta}\frac{\sqrt{3}}{2}\left[\frac{-3}{2}\frac{J_3}{J_2^{\frac{5}{2}}}S_{ij} + \frac{1}{J_2^{1.5}}\left(S_{ik}S_{kj} - \frac{2}{3}J_2\delta_{ij}\right)\right] \tag{A.6}$$

$$\frac{\partial \alpha}{\partial \sigma_{ij}} = X\kappa \sin\theta \frac{\sqrt{3}}{2\sin 3\theta}\left[\frac{-3}{2}\frac{J_3}{J_2^{\frac{5}{2}}}S_{ij} + \frac{1}{J_2^{1.5}}\left(S_{ik}S_{kj} - \frac{2}{3}J_2\delta_{ij}\right)\right] \tag{A.7}$$

Substituting the above equations (A.2), (A.3), (A.4) and (A.7) in to equation (A.1), we have

$$\frac{\partial f}{\partial \sigma_{ij}} = PS_{ij} + Q + R\delta_{ij} \tag{A.8}$$

$$P = \left[\frac{A}{(f_c')^2} + \frac{\alpha}{f_c'}\frac{1}{2\sqrt{J_2}} - \frac{3\sqrt{3}}{4f_c'}\frac{X\kappa\sin\theta}{\sin 3\theta}\frac{J_3}{J_2^2}\right] \tag{A.9}$$

$$Q = q * q_{ij} \tag{A.10}$$

$$q = -\frac{\sqrt{3}}{2f_c'}X\kappa\sin\theta\frac{1}{J_2\sin 3\theta} \tag{A.11}$$

$$q_{ij} = \left(S_{ik}S_{kj} - \frac{2}{3}J_2\delta_{ij}\right) \tag{A.12}$$

$$R = \left[\frac{B}{f_c'} + \frac{2C_0I_1}{(f_c')^2}\right] \tag{A.13}$$